

# Three Solution Approaches to Stochastic Multi-Period AC Optimal Power Flow in Active Distribution Systems

Muhammad Usman<sup>✉</sup>, Member, IEEE, and Florin Capitanescu<sup>✉</sup>, Member, IEEE

**Abstract**—This paper proposes three novel solution approaches (A1, A2, A3) to solve stochastic multi-period AC optimal power flow (S-MP-OPF) for day-ahead flexibility procurement from distributed energy resources (DER) in active distribution systems (ADSs). The S-MP-OPF is a mixed-integer nonlinear programming (MINLP) problem due to the binary variables modeling the operation of storage devices and flexible loads. The proposed three approaches have a shared common first step, which resorts to a new mixed-integer linear programming (MILP) model approximation of the S-MP-OPF problem. The MILP model employs second-order Taylor series expansion of trigonometric terms and formulates the linear approximations relying on variables such as square of voltage magnitude and voltage angle difference. This first step serves also the purpose of fixing the binary variables to the values computed by the MILP problem. Then, the approach A1 only checks the AC feasibility of MILP solution while approaches A2 and A3 further optimize continuous variables. Specifically, the sophisticated heuristic approach A2 employs sequential linear programming and AC power flow while the approach A3 models and solves directly the remaining nonlinear programming (NLP) problem. The performances of these approaches, a benchmark MINLP solver, and a state-of-the-art method are thoroughly compared in three radial or weakly meshed ADSs of 34, 31, and 191 nodes, respectively. The numerical results indicate that, albeit the approach A2 performs best overall, these approaches present distinct accuracy vs speed trade-offs, which make them suitable to problems of different sizes and diverse accuracy or speed requirements.

**Index Terms**—Active distribution systems, flexibility, multi-period optimal power flow, stochastic optimization, tractability.

## NOMENCLATURE

### Sets

- $N$  set of nodes.
- $G$  set of renewable energy sources (RES).
- $B$  set of electrical energy storages (EES).
- $F$  set of flexible loads (FLs).
- $E$  set of high voltage (HV)/medium voltage substations.

Manuscript received 6 April 2022; revised 28 July 2022; accepted 6 September 2022. Date of publication 8 September 2022; date of current version 19 December 2022. This work was supported by EU's Horizon 2020 Program under Grant 864298 (Project ATTEST). Paper no. TSTE-00346-2022. (*Corresponding author:* Florin Capitanescu.)

The authors are with the Luxembourg Institute of Science and Technology Belvaux, 4422 Belvaux, Luxembourg (e-mail: muhammad.usman@list.lu; fcapi@espace@yahoo.com).

Color versions of one or more figures in this article are available at <https://doi.org/10.1109/TSTE.2022.3205213>.

Digital Object Identifier 10.1109/TSTE.2022.3205213

$L/L^c$	set of lines/set of lines in a cycle.
$L^T$	set of on-load tap changing (OLTC) transformers.
$Y$	set of discrete values of OLTC transformer ratio.
$T/S$	set of time-periods/set of scenarios.

### Optimization Variables (in period $t$ and scenario $s$ )

$P_{i,s,t}^e$	active power flow from HV upstream grid at node $i$ .
$Q_{i,s,t}^e$	reactive power flow from HV upstream grid at bus $i$ .
$P_{i,s,t}^{curt}$	amount of RES curtailed active power at node $i$ .
$Q_{i,s,t}^{RES}$	reactive power provision from RES at node $i$ .
$P_{i,s,t}^{ch}$	active power charging of EES at node $i$ .
$P_{i,s,t}^{dch}$	active power discharging of EES at node $i$ .
$P_{i,s,t}^{od}$	active power overdemand of FL at node $i$ .
$P_{i,s,t}^{ud}$	active power underdemand of FL at node $i$ .
$\beta_{i,s,t}^{ch}$	binary variable modeling EES charging at node $i$ .
$\chi_{i,s,t}^{od}$	binary variable modeling FL overdemand at node $i$ .
$\mu_{if,s,t}^k$	binary variable modeling $k$ -th ratio of OLTC if.
$\lambda_{i,s,t}^k$	auxiliary variable modeling $\mu_{if,s,t}^k \cdot V_{i,s,t}^2$ .
$SoC_{i,s,t}$	State-of-Charge (SoC) of EES at node $i$ .
$V_{i,s,t}^2$	square of voltage magnitude at node $i$ .
$\theta_{ij,s,t}$	voltage angle difference between nodes $i$ and $j$ .

### Parameters (in period $t$ and scenario $s$ )

$g_{ij}$	conductance of the branch between buses $i$ and $j$ .
$b_{ij}$	susceptance of the branch between buses $i$ and $j$ .
$P_{i,s,t}^0$	available active power of RES unit at node $i$ .
$P_{i,s,t}^d/Q_{i,s,t}^d$	active/reactive power demand at node $i$ .
$\varphi_{i,s,t}$	angle defining load power factor $\cos(\varphi_{i,s,t})$ .
$\phi_{i,s,t}$	angle defining RES power factor $\cos(\phi_{i,s,t})$ .
$P_i^{ch,r}$	rated active power charging of EES at node $i$ .
$P_i^{dch,r}$	rated active power discharging of EES at node $i$ .
$E_i^r$	rated energy capacity of EES at node $i$ .
$\eta_i^{ch}/\eta_i^{dch}$	charging/discharging efficiency of EES at node $i$ .
$r_{if}^k$	$k$ -th discrete ratio value of OLTC if.
$\underline{x}/\bar{x}$	minimum/maximum value of $x$ (e.g., $V$ , $SoC$ ).
$\Delta T$	duration of time period $t$ .
$M$	demand flexibility factor as % of available load.
$c_{i,p}^{curt}$	cost (€ /MWh) of curtailed active power at node $i$ .

$c_{i,b}^{str}$	cost (€ /MWh) of storage usage at node $i$ .
$c_{i,l}^{fl}$	cost (€ /MWh) of demand flexibility at node $i$ .
$c_{ij}^{oltc}$	wear and tear cost (€) of OLTC transformer.
$\pi_s$	likelihood of uncertainty scenario $s$ .

## I. INTRODUCTION

### A. Motivation

The steady growing penetration of variable renewable energy sources (RES), mostly solar and wind, have transformed passive distribution networks into active distribution systems (ADSs) [1]. However, the variability of RES output can breach operation constraints (e.g., voltage rise or congestion [2]), hardening the distribution system operator (DSO) task of maintaining reliable ADS operation. To effectively counteract such issues, beyond adjustments of conventional ADS control means and RES, additional controllable distributed energy resources (DER) such as electrical energy storages (EESs) and flexible loads (FLs) can be installed in ADSs. The flexibility of these DER can be exploited by DSOs to maintain reliable and cost-effective ADS operation. In this context, it becomes crucial to operate ADSs optimally, exploiting their full flexibility potential. To this end, advanced ADS operation approaches, which address efficiently the needs and challenges of future ADSs, while being tractable, are highly needed.

The key requirement in future ADSs is the flexibility procurement by DSOs from DER to meet operation constraints. This can be adequately addressed under the framework of stochastic multi-period AC optimal power flow (S-MP-OPF) [3], as it captures key needs such as RES uncertainty and inter-temporality of DER. As such the DSO can utilize these resources in an optimal manner to meet the operation constraints. However, S-MP-OPF problem, in its full formulation, belongs to the class of mixed-integer non-linear programming (MINLP), which is not tractable for realistic practical problems. Therefore, to comply with the solution time requirement of DSOs (ideally 15–60 minutes in the frame of day-ahead operation planning), novel approaches which can provide the best possible solution in such a short time are need of the hour. *In this context, the main motivation of this work is to develop novel solution approaches, with different trade-off between accuracy and tractability, to S-MP-OPF problem of flexibility procurement by DSO in day-ahead operation planning.*

### B. Related Works

The consideration of RES and/or emerging DER, in day-ahead S-MP-OPF flexibility procurement framework in ADSs has been recently significantly researched [4], [5], [6], [7], [8], [9], [10], [11], [12], [13], [14], [15], [16], [17], [18], [19], [20]. However, such a framework belongs to the MINLP class whose computational bottleneck arises from: (i) binary variables modeling modern DER (EESs, FLs) and conventional assets (OLTC transformers), (ii) the large problem size, determined by the product of three dimensions: network size, number of uncertainty scenarios and number of time-periods, and (iii) the

non-convex AC power flow equations. Consequently, to reduce the computational burden of the MINLP model, simpler optimization models tackling non-convexity, problem dimension or both have been proposed, which are briefly reviewed hereafter. Note that the activation of procured flexibility in day-ahead is usually carried out by some *real-time* OPF algorithm [21], [22], [23], which falls outside the scope of this work.

The models proposed in [4], [5], [6], [7], [8] consider only the RES stochasticity but ignore the inter-temporal DER constraints, thus leading to stochastic single-period (S-SP) optimization problems. Conversely, [9], [10], [11] consider inter-temporal DER constraints but disregard RES stochasticity, resulting to deterministic multi-period (D-MP) optimization problems. As such, the above research lines neglect one salient *dimension* of future ADSs and solve a reduced dimension optimization model, which is incapable of *fully* representing the future ADSs.

To overcome the modeling limitations of the previous works [4], [5], [6], [7], [8], [9], [10], [11], more recent researches in [12], [13], [14], [15], [16], [17], [18], [19], [20] consider both inter-temporal and stochastic characteristics of DER and RES, respectively. However, either an intractable MINLP model is tackled [13], [14] or tractability is achieved using convex relaxations [15], [16] or approximation techniques [17], [18], [19], [20].

For instance, in [15], [16], the non-convexity of AC power flow equations is handled by second-order cone programming relaxation. However, there is no guarantee regarding the feasibility of recovered solution. In [17], [19], linear relation between the voltages and injected powers, originally proposed in [24], is utilized; however, losses terms are ignored in [24]. In [18], binary variables-based piece-wise linear terms are derived to replace the trigonometric functions, which inadvertently increases the integral dimension of model under a stochastic multi-period (S-MP) framework. Moreover, the adopted small voltage variation assumption in [18] does not hold under stressed operating conditions. Lastly, in [20], a linear energy balance equation is formulated but it ignores the non-linear power flow equations.

As regards flexible options employed, only a subset of flexible resources of future ADSs are modeled in [12], [13], [14], [15], [16], [17], [18], [19], [20], mainly focusing on using RES and EESs. Accordingly, other flexible assets such as FLs, reactive power provision from RES [12], [13], [14], [15], [16], [17], [18], [19] and OLTC transformer [12], [14], [17], [18], [19], [20] are ignored. Moreover, in the majority of works, EESs and FLs are modeled using an approximation of their intrinsic integer model by simply dropping the binary variables [9], [10], [11], [12], [13], [17].

Finally, the uncertainty modeling of DER in OPF framework are carried out by: stochastic [7], [8], [12], [14], [18], [19], [20], chance constrained [4], [17] or robust [5], [6], [13], [15] optimization techniques. Each of these approaches exhibits well known pros and cons; readers can refer to the above-mentioned works in each category for better understanding. This paper opts for stochastic optimization as the proposed algorithm can be fed with a reasonable number of scenarios without compromising its computation time.

TABLE I  
KEY FEATURES OF EXISTING WORKS

Ref.	Char.	Flexibility Resources		Model Formulation		
		Continuous	Discrete	Accurate	Approx.	Relaxation
[4], [6]	S-SP	RES	OLTC		MISOCP	
[5]	S-SP	RES			MISOCP	
[7]	S-SP	RES			SOCP	
[8]	S-SP	RES	FLs	MINLP		
[9]	D-MP	RES, FLs, EES, APF	OLTC		MILP	
[10]	D-MP	EES, FLs		NLP		
[11]	D-MP	RES, EES		NLP		
[12]	S-MP	RES, EES		NLP		
[13]	S-MP	RES, EES	OLTC	MINLP		
[14]	S-MP	RES	EES	MINLP		
[15]	S-MP	RES	EES, OLTC		MISOCP	
[16]	S-MP	RES, FLs	EES, OLTC		MISOCP	
[17]	S-MP	RES, EES		LP		
[18]	S-MP	RES		MILP		
[19]	S-MP	RES	EES	MILP		
[20]	S-MP	RES	EES, FLs	MILP		
This Work	S-MP	RES, APF	EES, FLs, OLTC	MILP		

Char.: characteristics, Approx.: approximation, APF: adaptive power factor

### C. Paper Contributions

The literature review allows safely concluding that the existing approaches do not consider all flexible options which can be envisioned in future ADSs as well as rely on convex relaxation or single-step linearization approaches to foster tractability. However, convex relaxations provide AC feasible solutions under stringent conditions [25], which usually do not hold in real-life ADSs. Also, since the explored linearization techniques are single step, generally based on small voltage deviation assumption around the linearization point, and fail to model the impact of losses, their solutions can be inaccurate under stressed operating conditions. These shortcomings are tackled in this paper through novel tractable approaches which provide highly accurate, near-optimal solution.

The main contributions of this work are the following:

- Three approaches (A1, A2, A3) with various trade-offs between solution accuracy and tractability are proposed. These approaches have a shared common first step, which resorts to a new mixed-integer linear programming (MILP) model of the S-MP-OPF problem. This first step serves also the purpose of fixing the binary variables to the values computed by the MILP problem. Then, the approach A1 only checks the AC feasibility of MILP solution (i.e., acts conceptually similarly to the majority of existing single-step linear techniques) while approaches A2 and A3 further optimize continuous variables. Specifically, the approach A2 employs sequential linear programming (SLP) and AC power flow, while the approach A3 models and solves directly the remaining nonlinear programming (NLP) problem.
- The MILP model which relies on novel second-order linear approximation of AC active/reactive power flow and branch current expressions. The proposed linear approximations are based on *square of voltage magnitude* and *voltage angle difference* variables, utilize second-order

Taylor series expansion of trigonometric terms and introduce a novel linearization of bi-linear voltage magnitude term. Moreover, the proposed approximations do not rely on extensively used flat/near voltage profile and small angle assumptions [26], [27], [28], [29]. As such, they capture more non-linearity than the existing works and implicitly model network losses and their dependency on both voltage magnitude and angle.

Note that these approximations were briefly tested in our paper [30] for a SP deterministic AC OPF with a limited number of flexible options and applied to a 34-bus radial ADS. In this paper, after demonstrating empirically their high accuracy for general-purpose application, these approximations are leveraged to S-MP-OPF with a comprehensive set of flexible options and tested on real-world larger, radial and weakly meshed, ADSs to showcase their versatility and scalability.

Finally, Table I summarizes the key aspects of the proposed framework, which distinguishes it from the existing works.

## II. BENCHMARK STOCHASTIC MULTI-PERIOD AC-OPF MINLP FLEXIBILITY PROCUREMENT FRAMEWORK

This section develops the MINLP benchmark model for flexibility procurement through S-MP-OPF in day-ahead operation planning of MV ADSs [3]. This framework assumes that the ADSs are sufficiently observable such that a centralized OPF computation can be contemplated in confidence by the DSO. The model computes optimal schedules that flexible DER (RES, EESs, FLs) need to track the next day to mitigate congestion or voltage issues. The real-time control during the next day may need to further minimize DER deviations from their day-ahead schedules; however this falls outside the scope of the paper.

Accordingly, the objective (1) minimizes the overall expected cost of network operation, expressed in terms of DER re-dispatch from the market schedule (not shown explicitly for formulation ease) in each time period  $t$  and scenario  $s$ :

$$\min \sum_{s \in S} \sum_{t \in T} \pi_s \left\{ \left( \sum_{i \in G} c_{i,p}^{curt} P_{i,s,t}^{curt} + \sum_{i \in B} c_{i,b}^{str} (P_{i,s,t}^{dch} - P_{i,s,t}^{ch}) \right. \right. \\ \left. \left. + c_{i,l}^{fl} \sum_{i \in F} (P_{i,s,t}^{od} + P_{i,s,t}^{ud}) \right) \Delta T + c_{ij}^{oltc} \cdot \kappa_{if,s,t} \right\} \quad (1)$$

The problem obeys the following constraints ( $\forall t \in T, s \in S$ ):

$$P_{i,s,t}^e + (P_{i,s,t}^0 - P_{i,s,t}^{curt}) + (P_{i,s,t}^{dch} + P_{i,s,t}^{ch}) - (P_{i,s,t}^d + P_{i,s,t}^p \\ - P_{i,s,t}^{ud}) = \sum_{ij \in L \cup L^T} P_{ij,s,t} \quad \forall i \in N \quad (2)$$

$$Q_{i,s,t}^e + Q_{i,s,t}^{RES} - \{Q_{i,s,t}^d + \tan(\varphi_{i,s,t})(P_{i,s,t}^{od} - P_{i,s,t}^{ud})\} \\ = \sum_{ij \in L \cup L^T} Q_{ij,s,t} \quad \forall i \in N \quad (3)$$

$$P_{ij,s,t} = g_{ij} V_{i,s,t}^2 - g_{ij} V_{i,s,t} V_{j,s,t} \cos(\theta_{ij,s,t}) \\ - b_{ij} V_{i,s,t} V_{j,s,t} \sin(\theta_{ij,s,t}) \quad \forall ij \in L \cup L^T \quad (4)$$

$$Q_{ij,s,t} = -b_{ij} V_{i,s,t}^2 + b_{ij} V_{i,s,t} V_{j,s,t} \cos(\theta_{ij,s,t}) \\ - g_{ij} V_{i,s,t} V_{j,s,t} \sin(\theta_{ij,s,t}) \quad \forall ij \in L \cup L^T \quad (5)$$

$$\underline{V}_i^2 \leq V_i^2 \leq \bar{V}_i^2 \quad \forall i \in N \quad (6)$$

$$(g_{ij}^2 + b_{ij}^2) \{V_{i,s,t}^2 + V_{j,s,t}^2 - 2V_{i,s,t}V_{j,s,t} \cos(\theta_{ij,s,t})\} \leq |\bar{I}_{ij}|^2 \quad \forall ij \in L \cup L^T \quad (7)$$

$$\underline{P}_i^e(Q_i^e) \leq P_{i,s,t}^e(Q_{i,s,t}^e) \leq \bar{P}_i^e(\bar{Q}_i^e) \quad \forall i \in E \quad (8)$$

$$0 \leq P_{g,s,t}^{curt} \leq P_{g,s,t}^0 \quad \forall g \in G \quad (9)$$

$$-\tan(\bar{\phi}_{i,s,t})(P_{i,s,t}^0 - P_{i,s,t}^{curt}) \leq Q_{i,s,t}^{RES} \leq \tan(\bar{\phi}_{i,s,t}) \quad (10)$$

$$0 \leq P_{l,s,t}^{od} \leq M \cdot P_{l,s,t}^d \cdot \chi_{l,s,t}^{od} \quad \forall l \in F \quad (11)$$

$$0 \leq P_{l,s,t}^{ud} \leq M \cdot P_{l,s,t}^d \cdot (1 - \chi_{l,s,t}^{od}) \quad \forall l \in F \quad (12)$$

$$\sum_{t \in T} P_{l,s,t}^{od} \cdot \Delta T = \sum_{t \in T} P_{l,s,t}^{ud} \cdot \Delta T \quad \forall l \in F \quad (13)$$

$$-\beta_{b,s,t}^{ch} \cdot P_b^{ch,r} \leq P_b^{ch} \leq 0 \quad \forall b \in B \quad (14)$$

$$0 \leq P_{b,s,t}^{dch} \leq (1 - \beta_{b,s,t}^{ch}) \cdot P_b^{dch,r} \quad \forall b \in B \quad (15)$$

$$SoC_{b,s,t} - SoC_{b,s,t-1} = \frac{\Delta T}{E_b^r} \left( -\eta_b^{ch} P_{b,s,t}^{ch} - \frac{P_{b,s,t}^{dch}}{\eta_b^{dch}} \right) \quad (16)$$

$$\underline{SoC}_b \leq SoC_{b,s,t} \leq \bar{SoC}_b \quad \forall b \in B \quad (17)$$

$$SoC_{b,s,t_n} = SoC_{b,s,t_0} \quad \forall b \in B \quad (18)$$

$$V_{f,s,t}^2 = \sum_{k=1}^Y r_{if}^k \times \lambda_{if,s,t}^k \quad \forall if \in L^T, k \in Y \quad (19)$$

$$\underline{V}_i^2 \cdot \mu_{if,s,t}^k \leq \lambda_{if,s,t}^k \leq \bar{V}_i^2 \cdot \mu_{if,s,t}^k \quad \forall if \in L^T, k \in Y \quad (20)$$

$$\underline{V}_i^2 \cdot (1 - \mu_{if,s,t}^k) \leq V_{i,s,t}^2 - \lambda_{if,s,t}^k \leq \bar{V}_i^2 \cdot (1 - \mu_{if,s,t}^k) \quad \forall if \in L^T, k \in Y \quad (21)$$

$$\sum_{k=1}^Y \mu_{if,s,t}^k = 1 \quad \forall if \in L^T, k \in Y \quad (22)$$

$$\left| \sum_{k=1}^Y \{r_{if}^k \cdot \lambda_{if,s,t}^k\} - r_{if,s,t}^0 \right| \leq \kappa_{if,s,t} \quad \forall if \in L^T, k \in Y \quad (23)$$

where the constraints of the above model have the following meaning: (2) and (3) express active and reactive power balance at buses, (4) and (5) represent the active and reactive power flows through branches, (6) limits voltage magnitude at buses, (7) limits the longitudinal current in branches, (8) bounds the active (reactive) power flow at the main substations, (9) models the active power curtailment of RES, (10) expresses reactive power output of RES, (11) and (12) limit the over- and under-demand of active power of FLs, (13) maintains the energy balance of FLs over the entire time horizon, (14) and (15) limit the active power charging and discharging of EESs, (16) models the EESs energy balance, (17) limits the *SoC* and (18) ensures that the *SoCs* on the first and last time periods are equal.

Constraints (19)–(22) model an OLTC transformer as an ideal transformer in series with the transformer impedance. The introduction of a fictitious node (*f*) leads to  $V_f^2 = r_{if}^2 V_i^2$ , which is handled by the standard product of binary-continuous variables

linearization approach [31], [32], leading to constraints (19)–(22). Note that any other existing technique such as [33] which transforms the OLTC non-linear equations into mixed-integer linear constraints can be used instead of (19)–(22). Lastly, (23) models the transformer operation cost term in the objective function. Note that in (2)–(23), all decision and control variables are treated as wait-and-see variables.

This MINLP formulation considers a comprehensive set of flexible options. However, in some ADSs, where FLs and EESs are not present and discreteness of OLTC is neglected, the problem becomes a NLP model. Lastly, the intractability of MINLP model stems from binary variables as well as non-linear constraints (4)–(7). To ensure tractability, an accurate approximation of the benchmark problem is developed in the next section, relying on the linear approximations of active/reactive power flows and branch currents.

### III. LINEARIZATION OF THE BENCHMARK MINLP MODEL

#### A. Linearized Active and Reactive Power Expressions

Observe that the non-linearity in active and reactive power flows equations, (4) and (5), stems from the quadratic term ( $V_i^2$ ), the bi-linear term ( $V_i V_j$ ) and the trigonometric terms  $\cos(\theta_{ij})$  and  $\sin(\theta_{ij})$ . Moreover, voltage magnitude and angle are tightly coupled in  $V_i V_j \cos(\theta_{ij})$  and  $V_i V_j \sin(\theta_{ij})$  terms. The proposed approximation tackles these non-linearities through the *second-order Taylor series* expansion of trigonometric terms and by transforming the bi-linear term as a function of the square of voltage magnitude. As such, it works in the space of two new independent variables: the *square of voltage magnitude* ( $V_i^2$ ) and *voltage angle difference* ( $\theta_{ij}$ ).

The first step of the proposed linearization technique substitutes the trigonometric terms in (4) and (5) with their second-order Taylor series expansion terms around the initial linearization point  $\theta_{ij}^{(0)}$ , leading to (the subscripts *s* and *t* are dropped hereafter for the sake of visibility):

$$\begin{aligned} P_{ij} &= (g_{ij} + g_{ij}^{sh}/2)(V_i^2) - (c_1 g_{ij} + s_1 b_{ij})V_i V_j \\ &\quad - (c_2 g_{ij} + s_2 b_{ij})V_i V_j \theta_{ij} - (c_3 g_{ij} + s_3 b_{ij})V_i V_j \theta_{ij}^2 \end{aligned} \quad (24)$$

$$\begin{aligned} Q_{ij} &= -(b_{ij} + b_{ij}^{sh}/2)(V_i^2) + (c_1 b_{ij} - s_1 g_{ij})V_i V_j \\ &\quad + (c_2 b_{ij} - s_2 g_{ij})V_i V_j \theta_{ij} + (c_3 b_{ij} - s_3 g_{ij})V_i V_j \theta_{ij}^2 \end{aligned} \quad (25)$$

where  $c_1 = s_2 + c_3 \theta_{ij}^{2(0)}$ ,  $s_1 = -c_2 + s_3 \theta_{ij}^{2(0)}$ ,  $c_2 = c^{(0)} \theta_{ij}^{(0)} - s^{(0)}$ ,  $s_2 = s^{(0)} \theta_{ij}^{(0)} + c^{(0)}$ ,  $c_3 = -\frac{c^{(0)}}{2}$ ,  $s_3 = -\frac{s^{(0)}}{2}$ ,  $c_0 = \cos(\theta_{ij}^{(0)})$ ,  $s_0 = \sin(\theta_{ij}^{(0)})$  and superscript *sh* denotes shunt.

To further decouple the three remaining non-linear terms ( $V_i V_j$ ,  $V_i V_j \theta_{ij}$  and  $V_i V_j \theta_{ij}^2$ ), the second step linearizes the last two non-linear terms via the first-order Taylor series expansion. To further decouple the three remaining non-linear terms ( $V_i V_j$ ,  $V_i V_j \theta_{ij}$  and  $V_i V_j \theta_{ij}^2$ ), the second step linearizes the last two non-linear terms via the first-order Taylor series expansion.

1) *Linearization of  $V_i V_j \theta_{ij}$  and  $V_i V_j \theta_{ij}^2$  Terms:* Considering  $V_i V_j$  and  $\theta_{ij}$  as two independent terms, the first-order Taylor

series expansion of  $V_i V_j \theta_{ij}$  and  $V_i V_j \theta_{ij}^2$  leads to:

$$V_i V_j \theta_{ij} \approx \theta_{ij}^{(0)} (V_i V_j) + V_i^{(0)} V_j^{(0)} (\theta_{ij} - \theta_{ij}^{(0)}) \quad (26)$$

$$V_i V_j \theta_{ij}^2 \approx \theta_{ij}^{2(0)} (V_i V_j) + 2V_i^{(0)} V_j^{(0)} \theta_{ij}^{(0)} (\theta_{ij} - \theta_{ij}^{(0)}) \quad (27)$$

These equations indicate that the coupling between the voltages magnitude and angles no longer exist and therefore the two terms under study can be approximated only in terms of  $\theta_{ij}$  variable. Next, by substituting (26)-(27) in (24)-(25), the remaining non-linearity appears only in  $V_i V_j$  term.

2) *Linearization of the  $V_i V_j$  Term:* The approximation of non-convex bi-linear term  $V_i V_j$  further affects the accuracy of linearized active and reactive power flows, and consequently, the choice of methods for its linearization is key. The majority of existing works [27], [28], [29], [34], uses either  $V_i V_j \approx 1$  approximation, based on flat/near-voltage profile assumption, or the first-order Taylor series expansion of this term. However, these approximations are increasingly inaccurate under distorted voltage profiles or stressed operating conditions. To obtain a more accurate linear approximation of this term, the following mathematical transformation is applied.

First  $V_i V_j$  is expressed in terms of  $V^2$  as follows:

$$V_i V_j = \frac{V_i^2 + V_j^2}{2} - \frac{(V_i - V_j)^2}{2} = \frac{V_i^2 + V_j^2}{2} - \frac{(\Delta V_{ij})^2}{2} \quad (28)$$

The first fraction is linear in terms of  $V^2$  and is able to approximate with good precision the bi-linear term because the second term involves the square of difference of voltage terms which, in general, is small provided the consecutive nodes voltages remain close to each other. However, under stressed operating conditions, this assumption may not hold; therefore it becomes imperative to linearize  $\Delta V_{ij}^2$  term as well. To this end, the term is first expressed in terms of  $V^2$ , as shown in (29), and then its approximation via first-order Taylor series around initial operating point  $V^{(0)}$  is carried out in (30).

$$\Delta V_{ij}^2 = \frac{(V_i + V_j)^2}{(V_i + V_j)^2} \Delta V_{ij}^2 \approx \frac{(V_i^2 - V_j^2)^2}{(V_i^{(0)} + V_j^{(0)})^2} \quad (29)$$

$$\Delta V_{ij}^2 \approx \frac{2(V_i^{(0)} - V_j^{(0)})(V_i^2 - V_j^2)}{(V_i^{(0)} + V_j^{(0)})} - (V_i^{(0)} - V_j^{(0)})^2 \quad (30)$$

Finally, substituting (30) into (28) leads to the linear approximation of  $V_i V_j$  in terms of  $V^2$ :

$$V_i V_j \approx \frac{(V_i^2 + V_j^2)}{2} - (V_i^{(0)} - V_j^{(0)})^2 \left\{ \frac{(V_i^2 - V_j^2)}{(V_i^{2(0)} - V_j^{2(0)})} - \frac{1}{2} \right\} \quad (31)$$

Note that the adoption in this work of the  $(V^2, \theta_{ij})$  variable space, instead of  $(V, \theta_{ij})$  space, allows to reduce the overall linearization error in (31), because it naturally captures more accurately the non-linearity of terms involving voltage magnitudes. For example,  $g_{ij}^2 V_i^2$  and  $b_{ij}^2 V_i^2$  terms become linear in  $(V^2, \theta_{ij})$  space and therefore the linearization of these terms is not required, which ultimately reduces the overall linearization error. On the other hand, the linearization of these terms is still required in  $(V, \theta_{ij})$  space.

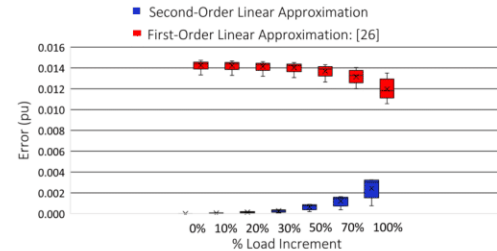


Fig. 1. Voltage errors by the two approximations.

3) *Linearized Active and Reactive Power Flows:* Based on (26)-(27) and (31), the linearized active and reactive power flows in terms of  $V^2$  and  $\theta_{ij}$  become:

$$P_{ij} = \alpha_i^P V_i^2 + \alpha_j^P V_j^2 + \beta_{ij}^P \theta_{ij} + \gamma_i^P \quad (32)$$

$$Q_{ij} = \alpha_i^Q V_i^2 + \alpha_j^Q V_j^2 + \beta_{ij}^Q \theta_{ij} + \gamma_i^Q \quad (33)$$

where  $\alpha_i^{P/Q}$ ,  $\alpha_j^{P/Q}$ ,  $\beta_{ij}^{P/Q}$ ,  $\gamma^{P/Q}$  are the coefficients of  $V^2$  and  $\theta_{ij}$  variables, which are reported in Table II.

### B. Linearized Longitudinal Branch Current Expression

The thermal loading on a branch  $ij$  can be expressed as:

$$|I_{ij}|^2 = (g_{ij}^2 + b_{ij}^2) \{V_i^2 + V_j^2 - 2V_i V_j \cos(\theta_{ij})\} \quad (34)$$

which is non-linear due to  $V^2$  and  $V_i V_j \cos(\theta_{ij})$  terms. As derived previously, the latter term can be linearized, in terms of  $V^2$ , via second-order Taylor series expansion of cosine term. Thus, using (31) leads to:

$$|I_{ij}|^2 = (g_{ij}^2 + b_{ij}^2) (\alpha_i^I V_i^2 + \alpha_j^I V_j^2 + \beta_{ij}^I \theta_{ij} + \gamma_i^I) \quad (35)$$

where  $\alpha_i^I$ ,  $\alpha_j^I$ ,  $\beta_{ij}^I$ ,  $\gamma^I$  are the coefficients of  $V^2$  and  $\theta_{ij}$  variables, which are reported in Table II. Note that, in this Table, the coefficients are reported under a S-MP framework i.e., parameters are derived for each scenario  $s$  and time period  $t$ .

### C. Sensitivity Analysis of the Proposed Second-Order Linear Approximations

To demonstrate the accuracy of derived second-order active and reactive power linear approximations, for general-purpose application, a sensitivity analysis is carried out, using, without loss of generality, the popular 34-bus test system [35].

In order to determine the performance of proposed approximations when operating conditions move away from the initial point of linearization, the active and reactive load at each node of the test system is increased till 100% of the initial load values and the obtained results (node voltages and branch current) from AC power flow based on i) non-linear AC power flow equations; ii) proposed second-order linear approximations (32)-(33), and iii) first-order linear approximations [26] are compared. In this regard, Figs. 1 and 2 show the calculated voltages and branch current error, where error is calculated as  $(|X_{nl}^i - X_{lin}^i| \forall i \in A)$  where  $X \in (V, I)$  and  $A = N$  or  $A = L$  depending upon the error being calculated. Note that the initial point of linearization is the base case active and reactive load values and in the

TABLE II  
COEFFICIENTS OF VARIABLES IN LINEARIZED ACTIVE & REACTIVE POWER FLOWS, AND LONGITUDINAL BRANCH CURRENT LIMIT EXPRESSION

Coefficients in $P_{ij}$ (32)		Coefficients in $Q_{ij}$ (33)		Coefficients in $I_{ij}$ (35)	
$\alpha_{i,s,t}^P$	$p_1 \frac{(3V_{j,s,t} - V_{i,s,t})}{2(V_{i,s,t} + V_{j,s,t})}$	$\alpha_{i,s,t}^Q$	$-p_2 \frac{(3V_{j,s,t} - V_{i,s,t})}{2(V_{i,s,t} + V_{j,s,t})}$	$\alpha_{i,s,t}^I$	$\frac{c_1 V_{i,s,t} + c_2 V_{j,s,t}}{(V_{i,s,t} + V_{j,s,t})}$
$\alpha_{j,s,t}^P$	$p_1 \frac{(3V_{i,s,t} - V_{j,s,t})}{2(V_{i,s,t} + V_{j,s,t})}$	$\alpha_{j,s,t}^Q$	$-p_2 \frac{(3V_{i,s,t} - V_{j,s,t})}{2(V_{i,s,t} + V_{j,s,t})}$	$\alpha_{j,s,t}^I$	$\frac{c_2 V_{i,s,t} + c_1 V_{j,s,t}}{(V_{i,s,t} + V_{j,s,t})}$
$\beta_{i,j,s,t}^P$	$p_2 V_{i,s,t} V_{j,s,t}$	$\beta_{i,j,s,t}^Q$	$p_1 V_{i,s,t} V_{j,s,t}$	$\beta_{i,j,s,t}^I$	$2s_{k-1} V_{i,s,t} V_{j,s,t}$
$\gamma_{i,s,t}^P$	$\{p_1(V_{i,s,t} - V_{j,s,t})^2/2\} - p_2 V_{i,s,t} V_{j,s,t} \theta_{ij,s,t}$	$\gamma_{i,s,t}^Q$	$\{-p_2(V_{i,s,t} - V_{j,s,t})^2/2\} - p_1 V_{i,s,t} V_{j,s,t} \theta_{ij,s,t}$	$\gamma_{i,s,t}^I$	$-2s_{k-1} V_{i,s,t} V_{j,s,t} \theta_{ij,s,t} - c_{k-1}(V_{i,s,t} - V_{j,s,t})^2$

$$p_1 = -c_{k-1} g_{ij} - s_{k-1} b_{ij}; p_2 = s_{k-1} g_{ij} - c_{k-1} b_{ij}; c_1 = 1 + c_{k-1}; c_2 = 1 - 3c_{k-1}$$

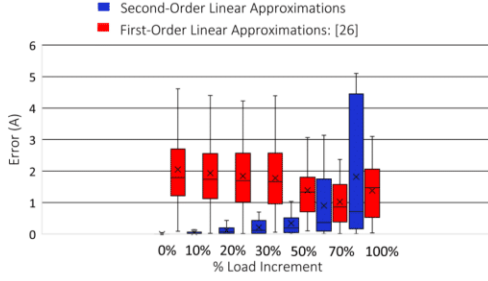


Fig. 2. Current errors by the two approximations.

subsequent (increasing load value) AC power flow run, the same power flow approximations, formulated around the initial point of linearization, are used.

The obtained results show that AC power flow under proposed second-order linear active and reactive power flow approximations provide highly accurate results in comparison to the AC power flow under first-order linear approximations, even when one moves significantly away from the initial point.

For voltages (see Fig. 1), the second-order approximation error remains significantly low in absolute terms and is also smaller than the first-order approximation error.

For branch currents (see Fig. 2), the similar trend is observed till 70% of load increment value after which first-order approximation error becomes lower than the second-order approximation error. However, we would like to emphasize that there is no guarantee about the accuracy of a particular approximation (since an approximation is supposed to work well only in the close vicinity of the point of linearization) when one moves significantly away from the point of linearization. Under such extreme circumstances, any approximation can work better than the other.

These results demonstrate empirically that the proposed second-order approximations capture better the non-linearity than the first-order linear approximations and as such are capable of providing more accurate results than its counterpart. Finally, the high accuracy of linear expressions, derived so far, enable a trustful development of some tractable approaches, presented hereafter, to S-MP-OPF problem.

#### IV. THE THREE PROPOSED APPROACHES

The three proposed approaches (A1, A2, A3) have a shared common first step, which resorts to a recursive MILP model approximation of the S-MP-OPF problem, based on the linear expressions derived in the previous section.

##### A. MILP Model Approximation of S-MP-OPF Problem

The proposed MILP model, expressed in  $V^2$  and  $\theta_{ij}$  variables, optimizes (1) under the constraints (2)–(3), (6), (8)–(23) and (36)–(42).

$$P_{ij,s,t} = \alpha_{i,s,t}^P V_{i,s,t}^2 + \alpha_{j,s,t}^P V_{j,s,t}^2 + \beta_{ij,s,t}^P \theta_{ij,s,t} + \gamma_{i,s,t}^P \quad \forall ij \in L \quad (36)$$

$$Q_{ij,s,t} = \alpha_{i,s,t}^Q V_{i,s,t}^2 + \alpha_{j,s,t}^Q V_{j,s,t}^2 + \beta_{ij,s,t}^Q \theta_{ij,s,t} + \gamma_{i,s,t}^Q \quad \forall ij \in L \quad (37)$$

$$P_{fj,s,t} = \alpha_{f,s,t}^P V_{f,s,t}^2 + \alpha_{j,s,t}^P V_{j,s,t}^2 + \beta_{fj,s,t}^P \theta_{fj,s,t} + \gamma_{f,s,t}^P \quad \forall f \in L^T \quad (38)$$

$$Q_{fj,s,t} = \alpha_{f,s,t}^Q V_{f,s,t}^2 + \alpha_{j,s,t}^Q V_{j,s,t}^2 + \beta_{fj,s,t}^Q \theta_{fj,s,t} + \gamma_{f,s,t}^Q \quad \forall f \in L^T \quad (39)$$

$$(g_{ij}^2 + b_{ij}^2)(\alpha_{i,s,t}^I V_{i,s,t}^2 + \alpha_{j,s,t}^I V_{j,s,t}^2 + \beta_{ij,s,t}^I \theta_{ij,s,t} + \gamma_{i,s,t}^I) \leq |I_{ij}|^2 \quad \forall ij \in L \quad (40)$$

$$\underline{\theta}_{ij,s,t} \leq \theta_{ij,s,t} \leq \bar{\theta}_{ij,s,t} \quad \forall ij \in L \cup L^T \quad (41)$$

$$\rho_{i,s,t}(V_{i,s,t}^2 + V_{j,s,t}^2) - v_{i,s,t}(V_{i,s,t}^2 - V_{j,s,t}^2) + \xi_{i,s,t} \geq 0 \quad \forall i, j \in N \quad (42)$$

where (36)–(37) and (38)–(39) represent the linear active and reactive power flows through a line and transformer, respectively, (40) models the linear branch current expression, (41) restricts the difference of voltage angles within defined bounds and (42) ensures the positivity of  $\Delta V_{ij}^2$ , where coefficients in (42) are defined as  $\rho_{i,s,t} = 1/2$ ,  $v_{i,s,t} = \frac{V_{i,s,t}^{2(0)} - V_{j,s,t}^{2(0)}}{V_{i,s,t}^{2(0)} + V_{j,s,t}^{2(0)}}$ ,  $\xi_{i,s,t} = (V_{i,s,t}^{2(0)} - V_{j,s,t}^{2(0)})^2/2$ .

This MILP model is valid for radial distribution systems only. For application to meshed networks, we add the following

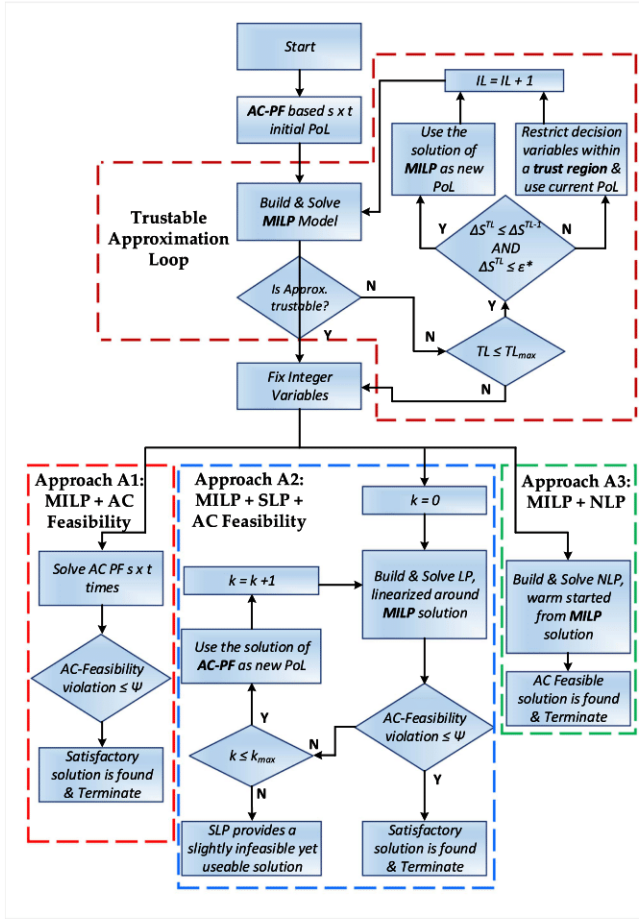


Fig. 3. Flowchart of the three proposed approaches.

constraint, which enforces the cyclic angle constraint (i.e., summation of voltage angle differences over each cycle in a mesh is zero):

$$\sum_{ij \in L^c} \theta_{ij,s,t} = 2n\pi \quad \forall ij \in L^c, n \in \mathbb{Z} \quad (43)$$

Note that linear active and reactive power flow expressions in  $(V^2, \theta_{ij})$  variables space [26] are obtained by resorting to their first-order Taylor series expansion, which results in completely different coefficients of  $V^2$  and  $\theta_{ij}$  variables than the ones presented in Table II. Our proposed model is compared against [26] in Section V.

### B. Description of the Proposed Approaches

Fig. 3 provides the flowchart of the three proposed approaches. One can observe that these approaches share the first step, which solves recursively the above MILP model approximation. This first step fixes, for subsequent steps, the binary variables, related to the modeling of EESs, FLs and OLTC ratio, to the values computed by the MILP problem.

The approach A1 only checks the AC feasibility of MILP solution via AC power flows, for each scenario  $s$  and time period  $t$ , and reports potential infeasibilities. It acts similarly to the

majority of existing single-step linear optimization techniques. Accordingly, this is the fastest approach but may not be able to satisfy AC constraints with desired accuracy  $\psi$ .

After fixing the binary variables, approaches A2 and A3 further optimize the continuous variables. The approach A2 employs sequential linear programming (SLP) and AC power flow (PF). More precisely, this approach linearizes the problem around the MILP solution and solves a linear programming (LP) problem. At the latter's solution, an AC power flow is performed for each scenario  $s$  and time period  $t$  to check the feasibility of the solution. This process is repeated until all AC constraints are satisfied within the desired accuracy  $\psi$ .

The approach A3 models and solves directly the remaining nonlinear programming (NLP) problem, using as warm-start the initial MILP solution. This approach does not require iterations since AC constraints are modeled and thereby met by default at the solution of the NLP problem.

Note that the MILP model approximation is improved recursively, in a trustable loop approximation (44), if MILP model solution moves towards the optimal solution i.e., if criteria  $\Delta S^{TL} < \Delta S^{TL-1}$  and  $\Delta S \leq \epsilon^*$  ( $\epsilon^* > \epsilon$ ) are satisfied. As such, MILP model solution is used as a new point of linearization (PoL). However, if these criteria are not satisfied, it indicates that MILP solution either moves away or is far from the optimal solution. In such a case, the decision variables are restricted within a trust region, MILP model is solved again and PoL is updated at its solution.

Furthermore, note that during the calculation of *initial s × t* PoL through AC PF, only RES available active power is considered as the values of control variables (RES curtailment, charging and discharging active power of EESs, and over/under-demand of active power of FLs) are not known beforehand in the first iteration. Consequently, the quality of *initial s × t* PoL may be affected; depending on the number and values of EESs and FLs. However, during subsequent iterations, the values of control variables, recovered from MILP model, are utilized while determining the new *s × t* PoL. Consequently, the quality of PoL and, in turn, the accuracy of MILP model is improved remarkably.

### C. Trustable Approximation Criterion

The normalized relative difference between the non-linear apparent power injection  $S^{nl}$  (determined by injecting the solution of MILP model in (4) and (5)) and linear apparent power injection  $S^{lin}$  at each node, calculated over the whole time horizon and uncertainty scenarios, is chosen as the trustable approximation criterion (44).

$$\Delta S_i = \max \left\{ \frac{\sum_{s \in S} \sum_{t \in T} S_{s,t,i}^{nl} - \sum_{s \in S} \sum_{t \in T} S_{s,t,i}^{lin}}{S \times T \times \max \left( \sum_{s \in S} \sum_{t \in T} S_{s,t,i}^{nl} \right)} \right\} \quad \forall i \in N \quad (44)$$

The satisfaction of approximation criterion ( $\Delta S \leq \epsilon$ ) ensures that the probability of the obtained MILP solution to lie in the

TABLE III  
INSTALLED DER AND LOAD DEMAND IN THE THREE TEST CASES

Test Cases	RES		EESs		FLs <sup>+</sup>		Peak Load	
	No.	Cap. (MW)	No.	Cap. (MW)	No.	P (MW)	Q (MVAr)	
34-bus	8	0.5/1	3	1	2	3.71	2.30	
UK 31-bus	8	2.6	3	1	4	6.51	2.14	
PT. 191-bus	23	2.0	10	1	20	18.75	6.16	

Cap: Capacity is defined per DER

<sup>+</sup> Flexibility from each FL is taken as 50% of its total demand

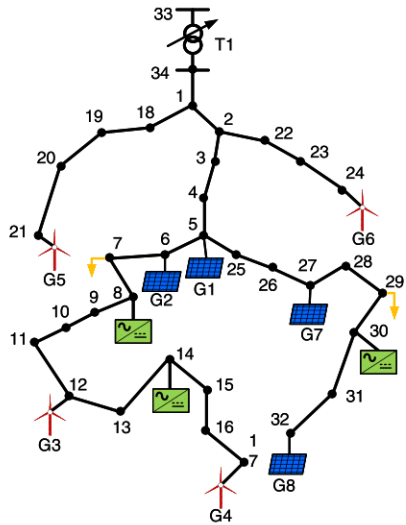


Fig. 4. Layout of modified 34-bus active distribution system.

close vicinity of the benchmark solution is quite high. Resultantly, the optimality gap can be zero or negligible.

## V. NUMERICAL RESULTS

### A. Description of Datasets and Simulation Settings

The performance of the three proposed approaches are evaluated on the modified, DER-rich, versions of following ADSs (see Table III for the characteristics of assumed DER):

- 34-bus 12.66 kV radial ADS [3]; (see Fig. 4)
- 30-bus 11 kV weakly-meshed real UK ADS [36];
- 191-bus 30 kV radial real Portuguese ADS [36].

The simulations assume 24 time-periods (i.e., hourly resolution of the day-ahead which is reasonable for day-ahead operation planning framework) as well as 10 uncertainty scenarios to case solar and wind RES stochasticity. These scenarios are generated using the well-established ARIMA model, whose details are provided in [3]. The maximum trustable approximation loop iteration is set to 2, whereas the trustable approximation criterion ( $\epsilon$ ) is set to  $1 \times 10^{-3}$  pu in order to restrict the error value, i.e., (44), below 1 kVA in all test cases. The AC feasibility threshold ( $\psi$ ) is set to 1% i.e., the value of nodes voltages and/or branch current above 1% of their rated pu values is considered as an infeasible solution in this work. Finally, the benchmark MINLP approach, called A0, and the three approaches are developed in Julia/JuMP [37] and are solved using Bonmin (for MINLP), CPLEX (for MILP and LP) and IPOPT (for NLP).

### B. Flexibility Options

The performances, in terms of accuracy and speed, of the three approaches and the benchmark A0 are assessed for nine distinct combinations of flexible options (FOs), called FO1-FO9, under different operating conditions. These FOs are: active power curtailment (APC-FO1) and various combinations of APC with (i) OLTC transformer (FO2), (ii) adaptive power factor (APF-FO3), (iii) OLTC and APF (FO4), (iv) EESs (FO5), (v) FLs (FO6), (vi) EESs and FLs (FO7), (vii) EESs, FLs and APF (FO8) and (viii) EESs, FLs, APF and OLTC (FO9). For FOs involving APF, the power factor of RES is allowed to vary between 0.90 lagging and 0.90 leading.

### C. Results for 34-Bus ADS

The performance of proposed approaches is assessed under hard conditions by setting up a stressed virtual operating point. At this point, the total number of *initial* voltage violations (i.e., above the feasibility threshold  $\psi > 1\%$ ) in all uncertainty scenarios over whole time-horizon is 310 while the maximum violation is 12.4% larger than the upper voltage bound.

Table IV provides the performance of the three proposed approaches in terms of optimality gap, potential constraint violations and calculation time. The optimality gap is defined as  $|\frac{A0^{obj} - Ax^{obj}}{A0^{obj}}|$  where  $A0^{obj}/Ax^{obj}$  is the optimal solution obtained after solving approaches  $A0/Ax$  where  $x \in (1, 2, 3)$ . The smaller the value of optimality gap, the closer the solution of proposed approaches to the benchmark optimal solution. Note that in FOs where A0 does not terminate in the maximum time limit, the best objective value obtained that far is used to calculate the optimality gap.

1) *Approaches Accuracy:* In terms of optimality, the approach A2 performs best as the optimality gap remains below 0.1% for all FOs, while for five FOs the gap is zero. This means that this approach converges to the same solution as the benchmark approach A0 and therefore achieves excellent accuracy as regards optimality. The approach A1 comes second, albeit it achieves small sub-optimality, i.e., below 0.22%. The approach A3 either converges to the same solution as the benchmark A0 or, in three cases, provides larger sub-optimal solutions, up to 1.87% for FO2.

In terms of constraints satisfaction, both approaches concerned by this criterion, A1 and A2, lead to AC feasible solutions. As such, the maximum reported violation for every FO is negligible (e.g., roughly  $2 \times 10^{-4}$  pu) and almost 100 times smaller than the AC feasibility threshold ( $\psi \leq 1\%$ ). Accordingly, the monitored violations are rather numerical errors in the range of solver convergence tolerance than actual violations. For A3, NLP converges and an AC feasible solution is obtained in all FOs.

The above results show also that single-step linear approaches widely used in the literature, like A1, can be indeed accurate in a number of cases. However, under stringent operating conditions, such an approach might lead to an AC infeasible solution as shown in the latter sections for 30-bus and 191-bus real world ADSs.

TABLE IV  
PERFORMANCE OF PROPOSED TRACTABLE APPROACHES IN 34-BUS ADS AND COMPARISON WITH THE BENCHMARK MINLP APPROACH

FOs	Optimality gap (%)			Constraints Violations						Computational Time (s)			
				Approach A1			Approach A2						
	A1	A2	A3	Nb.	Max (%)	$\leq 1\%$	Nb.	Max (%)	$\leq 1\%$	A0	A1	A2	A3
<b>FO 1</b>	0.02	0.02	0.00	0	$2.60 \times 10^{-4}$	0	0	$2.60 \times 10^{-4}$	0	16.4	0.9	1.4	17.1
<b>FO 2</b>	0.00	0.00	1.87	0	$2.53 \times 10^{-4}$	0	0	$2.53 \times 10^{-4}$	0	3600*	1.8	2.4	255.1
<b>FO 3</b>	0.05	0.00	0.00	0	$2.61 \times 10^{-4}$	0	0	$2.61 \times 10^{-4}$	0	20.9	0.8	1.2	16.1
<b>FO 4</b>	0.07	0.00	0.34	0	$2.54 \times 10^{-4}$	0	0	$2.64 \times 10^{-4}$	0	3600*	2.4	3.1	23.0
<b>FO 5</b>	0.00	0.00	0.00	0	$2.60 \times 10^{-4}$	0	0	$2.30 \times 10^{-4}$	0	94.3	2.1	2.5	25.6
<b>FO 6</b>	0.02	0.02	0.00	0	$2.45 \times 10^{-4}$	0	0	$2.46 \times 10^{-4}$	0	33.7	1.1	1.5	16.6
<b>FO 7</b>	0.00	0.00	0.00	0	$2.45 \times 10^{-4}$	0	0	$2.29 \times 10^{-4}$	0	93.4	2.3	2.8	37.5
<b>FO 8</b>	0.20	0.07	0.00	0	$2.58 \times 10^{-4}$	0	0	$2.62 \times 10^{-4}$	0	71.6	2.5	3.0	40.8
<b>FO 9</b>	0.22	0.03	0.33	0	$2.54 \times 10^{-4}$	0	0	$2.82 \times 10^{-4}$	0	3600*	4.2	4.8	70.7

A0 = MINLP; A1 = MILP + AC Feasibility; A2 = MILP + SLP + AC Feasibility; A3 = MILP + NLP

\*: maximum time execution limit reached in MINLP solver

TABLE V  
BASE CASE: WEAKLY MESHED UK 31-BUS ADS

FOs	Optimality Gap (%)			Computational Time (s)			
	A1	A2	A3	A0	A1	A2	A3
<b>FO 1</b>	0.03	0.03	0.03	16.4	1.8	2.0	21.4
<b>FO 4†</b>	0.41	0.05	0.13	3600*	9.7	11.8	42.7
<b>FO 4‡</b>	0.21	0.12	0.12	94.3	6.3	6.8	31.4
<b>FO 7</b>	0.06	0.07	0.06	93.4	4.8	5.9	55.6
<b>FO 9†</b>	0.41	0.19	0.01	71.6	5.5	6.7	43.5
<b>FO 9‡</b>	0.41	0.18	0.00	3600*	5.9	6.8	49.8

\*: maximum time execution limit reached in MINLP solver

2) *Approaches Speed:* In terms of computation time, the approach A1 is obviously the fastest, the approach A2 is only slightly less fast (due to the additional LP problem solved). It is observed that all FOs require one SLP iteration in the approach A2 before returning a feasible solution. Hence, the solution time of A2 is slightly higher than the solution time of A1. On the other hand, both A1 and A2 approaches are much faster (i.e., roughly 10 to 100 times) than the approach A3. The latter is still generally considerably faster than the benchmark A0, which reaches the maximum time execution limit, set to 3600 seconds, in three FOs. As such, MINLP solver does not return any integer solution and provides only a utopian lower bound, obtained as the solution of NLP relaxation in the first stage of MINLP algorithm, on the optimal value.

The above considerations indicate that the approach A2 leads to the best trade-off between accuracy and speed, closely followed by approach A1. From now on, the scalability and the versatility of all approaches are demonstrated on two real-world ADSs for a reduced number of flexible options.

#### D. Results for 30-Bus Weakly-Meshed UK ADS

The performance of the proposed approaches is evaluated in two cases (i) base case (original limits) and (ii) stressed operating conditions (thermal limit is reduced on three branches by 20%). The obtained results are reported in Tables V and VI. The ADS is initially congested during 17 and 24 instances in these cases,

respectively and the maximum overload is 44.8% above the rated thermal limit in both cases. Voltage violations are not observed in any simulation for this ADS. Lastly, FOs 4 and 9 are studied for two sets of taps, having 9 and 17 number of taps, to evaluate the performance of the MILP solver for larger combinatorial spaces.

1) *Approaches Accuracy and Speed in Base Case:* The conclusions drawn for the 34-bus ADS regarding approaches' performance hold here as well with the following exceptions: (i) Approaches A2 and A3 exhibit the best and equally good optimality, outperforming the approach A1, and (ii) the gap in the calculation time between approaches A1/A2 and A3 diminished significantly (A2 requires one SLP iteration in all FOs). However, the approach A2 still presents the best trade-off between accuracy and computation time. In terms of AC feasibility, no overloading violations are observed and as such, both approaches, A1 and A2, provide AC feasible results.

2) *Approaches Accuracy and Speed in the Stressed Case:* The results indicate primarily the limitation of single-step linearization of the approach A1 to maintain feasibility under stressed operating conditions, with 2 constraints violations larger than the acceptance threshold in FO9. All AC infeasible cases are shown with bold numbers in the table VI. On the other hand, thanks to further linearization, the approach A2 is capable of ensuring AC feasibility for the given threshold, although several slight violations (but acceptable given the chosen threshold) of up to 0.77% (and 0.22% in average) occur for all FOs. As such, the approach A2 provides the best objective and is much faster than the approach A3 at the expense of some slight but tolerable constraints violations. Lastly, A2 converges to a feasible solution for all FOs in one SLP iteration except FO9 which requires two iterations.

#### E. Results for 191-Bus Portuguese ADS

The three approaches are tested for the following two cases (i) base case (original limits) and (ii) stressed operating conditions (thermal limit is reduced on three branches by 20%). This ADS is initially congested during 6 and 27 instances in these cases, respectively and the maximum overload values are 11% and

TABLE VI  
STRESSED CASE: WEAKLY MESHED UK 31-BUS ADS

FOs	Optimality Gap (%)			Constraints Violations								Computational Time (s)					
				Approach A1				Approach A2									
	A1	A2	A3	Nb.	Max. (%)	Avg. (%)	$\leq$ Avg	$\leq$ 1%	Nb.	Max. (%)	Avg. (%)	$\leq$ Avg	$\leq$ 1%	A0	A1	A2	A3
<b>FO 1</b>	0.00	0.00	0.00	4	0.38	0.15	3	4	9	0.38	0.06	6	9	16.4	1.5	2.2	28.6
<b>FO 4<sup>†</sup></b>	0.43	0.01	0.30	11	0.48	0.15	8	11	2	0.43	0.41	1	2	3600*	7.1	7.9	45.3
<b>FO 4<sup>‡</sup></b>	0.44	0.14	0.14	4	0.04	0.02	2	4	3	0.05	0.02	1	3	94.3	4.1	5.0	131.1
<b>FO 7</b>	0.15	0.14	0.14	9	0.26	0.13	5	9	8	0.71	0.17	6	8	93.4	3.9	5.1	44.2
<b>FO 9<sup>†</sup></b>	0.48	0.05	0.13	13	<b>1.61</b>	0.49	10	11	8	0.77	0.22	6	8	71.6	15.5	19.7	60.8
<b>FO 9<sup>‡</sup></b>	0.69	0.04	0.48	13	<b>1.61</b>	0.49	10	11	8	0.77	0.22	6	8	3600*	9.7	12.8	61.5

\*: maximum time execution limit reached in MINLP solver

TABLE VII  
BASE CASE: RADIAL PT 191-BUS ADS

FOs	Optimality Gap (%)			Constraints Violations								Computational Time (s)					
				Approach A1				Approach A2									
	A1	A2	A3	Nb.	Max. (%)	Avg. (%)	$\leq$ Avg	$\leq$ 1%	Nb.	Max. (%)	Avg. (%)	$\leq$ Avg	$\leq$ 1%	A0	A1	A2	A3
<b>FO 1</b>	0.01	0.01	0.00	0	0.00	0.00	0	0	0	0.00	0.00	0	0	450.7	19.8	20.4	464.3
<b>FO 4<sup>†</sup></b>	0.24	0.02	0.02	1	0.18	0.18	0	1	1	0.18	0.18	0	1	3600*	88.7	107.1	641.9
<b>FO 4<sup>‡</sup></b>	0.28	0.04	0.05	1	0.60	0.60	0	1	1	0.59	0.59	0	1	3600*	87.4	153.4	1000.0
<b>FO 7</b>	0.11	0.10	0.09	3	0.10	0.06	2	3	4	0.01	0.01	2	4	3600*	44.7	53.2	801.9
<b>FO 9<sup>†</sup></b>	0.59	0.01	0.00	2	0.16	0.11	1	2	2	0.04	0.04	1	2	3600*	134.3	144.4	470.5
<b>FO 9<sup>‡</sup></b>	0.83	0.00	0.00	3	0.56	0.26	2	3	0	0.00	0.00	0	0	3600*	297.3	317.3	953.4

\*: maximum time execution limit reached in MINLP solver

TABLE VIII  
STRESSED CASE: RADIAL PT 191-BUS ADS

FOs	Optimality Gap (%)			Constraints Violations								Computational Time (s)					
				Approach A1				Approach A2									
	A1	A2	A3	Nb.	Max. (%)	Avg. (%)	$\leq$ Avg	$\leq$ 1%	Nb.	Max. (%)	Avg. (%)	$\leq$ Avg	$\leq$ 1%	A0	A1	A2	A3
<b>FO 1</b>	0.01	0.00	0.01	16	0.64	0.13	14	16	12	0.63	0.11	10	12	429.1	12.1	18.4	304.0
<b>FO 4<sup>†</sup></b>	0.32	0.03	0.02	12	<b>3.03</b>	0.58	10	10	10	0.71	0.22	7	10	3600*	58.8	65.2	962.2
<b>FO 4<sup>‡</sup></b>	0.21	0.00	0.00	11	0.27	1.13	6	11	9	0.23	0.07	7	9	3600*	64.0	71.7	754.2
<b>FO 7</b>	0.15	0.07	0.07	13	0.21	0.08	8	13	13	<b>1.14</b>	0.10	11	12	3600*	41.9	85.0	1428.1
<b>FO 9<sup>†</sup></b>	0.96	0.02	0.01	11	<b>1.40</b>	0.47	8	8	8	0.47	0.20	5	8	3600*	205.4	211.5	533.0
<b>FO 9<sup>‡</sup></b>	0.60	0.02	0.03	14	0.44	0.17	9	14	9	0.16	0.04	7	9	3600*	225.7	244.1	1117.3

\*: maximum time execution limit reached in MINLP solver

36% above the rated thermal limit in both cases. Additionally, no voltage violations are observed in these cases.

1) *Approaches Accuracy and Speed in Base Case:* Distinct results from the presented observations regarding ADS operation in base case are that the approaches A2 and A3 provide almost the equally good optimal solution and outperform A1 in terms of optimal solution. Moreover, both approaches, A1 and A2, converges to solutions with some very slight (but tolerable) violations, the largest being 0.60%. All approaches take expectedly consistently more time for this larger network, fact which will be discussed later on. The approach A2 necessitates substantial larger time than the approach A1, which is due to successive solutions of LP problem.

2) *Approaches Accuracy and Speed in the Stressed Case:*

Due to the further stressed conditions, approach A1 produces AC infeasible solutions in two cases (FOs 4<sup>†</sup> and 9<sup>†</sup>). The approach

A2 provides for the first time an infeasible solution, with a slight limit violation of 1.14% in FO7 instance.

Finally, as regards scalability, by comparing table VII-VIII one can observe that the computation time of the three approaches increases in average super-linearly with the problem size. However, the calculation time of the approaches A2 and A3, their largest time being around 5 minutes and 24 minutes respectively, can be safely contemplated for application in day-ahead operation planning for networks of comparable size. The approach A0 is expectedly intractable for such a large problem, and as such, fails to converge in the maximum allotted time.

#### F. Further Scalability Tests

Table IX explores further the scalability of proposed approaches for increasing number of scenarios and time-periods

TABLE IX  
SCALABILITY FOR INCREASED NUMBER OF SCENARIOS AND TIME-PERIODS

Sc.	24 time-periods			96 time-periods		
	Time (s)			Time (s)		
	A1	A2	A3	A1	A2	A3
10	226	244	1117	1366	1532	2879
20	356	381	1712	7138	8399	*
30	646	763	4146	14928	17728	*
40	992	1044	8972	**	**	**
50	1488	1575	*	**	**	**

Sc. = Number of Scenarios; \*: MUMPS runs out of memory

\*\*: CPLEX runs out of memory

(the two main factors affecting the problem size) for PT-191 bus ADS in the largest instance FO9<sup>‡</sup>. Note that solution time increases almost linearly with the problem size for approaches A1 and A2 under 24 time-periods. For approach A3, the solution time increases more than linearly with the problem size. For instance, the problem size increases by 4 times from 10 to 40 scenarios under 24 time-periods while the solution time grows 8 times. On the other hand, under 96 time-period, approaches A1 and A2 solution time grows exponentially with increasing problem size till 30 scenarios, whereas approach A3 only provides a feasible solution for 10 scenario case. For all the other scenarios, either CPLEX (A1 and A2) or MUMPS (A3) runs out of memory and as such, no solution is obtained.

One can conclude that the computation time for A1 and A2 is moderate and hence compatible with the day-ahead operation application (i.e., less than one hour) for a problem which is 5 times larger (50 scenarios and 24 time-periods) than the base case (10 scenarios and 24 time-periods). However, for the same problem size, A3 experiences a large computational time and is almost 5-9 times slower than A1 and A2. For problems beyond this problem size, the optimal solution is obtained approximately in 2-4 hours (scenarios 20–30 under 96 time-periods) for A1 and A2, which could be deemed still acceptable in day-ahead operation planning, whereas no solution is obtained for A3 under the same settings due to the limitation of the solver of handling a problem of large size.

Based on these results, it can be extrapolated that the proposed approaches, A1/A2 and A3, are scalable to ADSs which are at least 5 ( $\approx 1000$  nodes) and 3 ( $\approx 600$  nodes) times larger, respectively than the studied PT-191 bus network, and can provide an optimal solution in a time which is reasonable to DSOs in day-ahead operation framework.

#### G. Comparison With Method in [26] for S-MP-OPF

Table X shows the performance of *hot-start* linear power flow expressions [26] based S-MP-OPF model for PT-191 ADS operating under stressed condition. In terms of optimality gap, one observes that [26] leads to a slightly higher optimality gap than all three proposed approaches (see Table VIII).

In terms of solution feasibility, [26] provides an AC infeasible solution in FOs 4<sup>†</sup>, 4<sup>‡</sup>, 9<sup>†</sup> and 9<sup>‡</sup> as maximum constraint violation value becomes significantly higher than the thermal loading limit. The proposed approaches A2 and A3, on the other hand, provide AC feasible solution for these FOs, whereas A1 provides

TABLE X  
PERFORMANCE OF LINEARIZATION METHODOLOGY [26] FOR S-MP OPF

FOs	Optimality Gap (%)			Constraint Violation				Time (s)				
	A1	A2	A3	A1	Nb	Max (%)	A2	Nb.	Max (%)	A1	A2	A3
FO 1	0.01	0.01	0.01	16	0.64	16	0.64	12	12	310		
FO 4 <sup>†</sup>	0.38	0.04	0.31	21	<b>7.22</b>	18	0.22	76	79	980		
FO 4 <sup>‡</sup>	0.36	0.36	0.26	22	<b>7.76</b>	18	0.27	70	78	861		
FO 7	0.06	<b>IF</b>	0.14	11	0.21	<b>IF</b>	<b>IF</b>	52	<b>IF</b>	1130		
FO 9 <sup>†</sup>	0.50	0.03	0.58	19	<b>9.14</b>	16	0.42	245	262	975		
FO 9 <sup>‡</sup>	0.50	0.03	0.73	19	<b>9.14</b>	15	0.42	291	297	1136		

IF: MILP model becomes infeasible; Nb = Number

AC infeasible solution in two, instead of four, instances (FOs 4<sup>‡</sup> and 9<sup>†</sup>). However, the maximum violation values in A1 is significantly lower than the violation value of [26]. In terms of computational time, [26] takes slightly more time than the proposed approaches.

To conclude, the linear power flow expressions in [26] compare less favorably to the proposed approaches, the latter capturing better model non-linearity. This is mainly due to the first-order Taylor series expansion of power flow expressions, whereas proposed linear expressions in this work are based on the second-order Taylor series expansion of trigonometric terms and novel linearization technique for  $V_i V_j$  term.

#### H. Comparison of Proposed Approaches With Mixed-Integer Second-Order Cone Programming Approach

This section compares the performance of proposed approaches with state-of-the art mixed integer second-order cone programming (MISOCP) S-MP-OPF model [38], solved using CPLEX, under two objective functions: namely, minimization of active power losses (new objective function used only for the sake of comparison) in Table XI, and flexibility procurement objective (1) in Table XII under a range of flexible options. Moreover, the global optimality of proposed approaches solution is also numerically demonstrated.

In the case of active power losses minimization function, it can be seen in Table XI that MISOCP approach provides an AC feasible solution only in the case of UK 31-bus ADS under FOs 1 and 7, and PT 191-bus ADS under FO1 as the relaxation holds<sup>1</sup> in these cases. In all other FOs for these ADSs, CPLEX fails to solve the MISOCP approach in the allotted time and no integer solution is found. Similarly, in the case of 34-bus ADS, the relaxation fails to hold as can be noticed by AC infeasible solution (unrealistic voltage values are obtained which severely violate the voltage bounds). As such, the obtained solution represents a lower bound (of unknown tightness) to the objective value and does not have any physical meaning.

On the other hand, all three proposed solution approaches provide AC feasible and optimal solution under all FOs in all test cases, except A1 which leads to slightly AC infeasible solution in the case of PT 191-bus ADS under FOs 4, 7 and 9. Nevertheless, the observed violations are still within 2% of the maximum

<sup>1</sup>In [38], the constraint  $c_{ij}^2 + s_{ij}^2 = c_{ii} * c_{jj}$  is relaxed as  $c_{ij}^2 + s_{ij}^2 \leq c_{ii} * c_{jj}$  and relaxation error is defined as  $|c_{ij}^2 + s_{ij}^2 - c_{ii} * c_{jj}|$ .

TABLE XI  
COMPARISON OF THE PROPOSED APPROACHES WITH STATE-OF-THE-ART MISCOP [38] UNDER ACTIVE POWER LOSSES OBJECTIVE FUNCTION

FOs	Optimality Gap (%)				Constraint Violations												Computational Time (s)				
					MISOCP				A1				A2								
	MISOCP	A1	A2	A3	Nb.	Max (%)	Avg. (%)	≤ 1%	Nb.	Max (%)	Avg. (%)	≤ 1%	Nb.	Max (%)	Avg. (%)	≤ 1%	A0	MISOCP	A1	A2	A3
<b>34-bus ADS</b>																					
FO1	<b>4.6</b>	0.0	0.0	0.0	6820	<b>4.68</b>	2.66	826	0	$2.60 \times 10^{-4}$	$8.38 \times 10^{-5}$	0	0	$2.60 \times 10^{-4}$	$8.88 \times 10^{-5}$	0	37	5	2	3	4
FO4	<b>3.6</b>	0.3	0.2	0.0	7285	<b>4.66</b>	2.92	657	0	$2.53 \times 10^{-4}$	$1.13 \times 10^{-4}$	0	0	$2.53 \times 10^{-4}$	$1.38 \times 10^{-4}$	0	112	18	3	4	27
FO7	<b>3.5</b>	0.4	0.3	0.0	7185	<b>4.68</b>	2.66	720	0	$2.03 \times 10^{-4}$	$8.23 \times 10^{-5}$	0	0	$2.26 \times 10^{-4}$	$8.73 \times 10^{-5}$	0	85	21	5	6	35
FO9	<b>3.7</b>	0.8	0.5	0.0	5094	<b>2.35</b>	1.29	1835	0	$2.24 \times 10^{-4}$	$9.95 \times 10^{-5}$	0	0	$2.50 \times 10^{-4}$	$1.02 \times 10^{-4}$	0	130	22	5	6	33
<b>UK 31-bus ADS</b>																					
FO1	0.8	0.8	0.8	0.7	0	0	0	0	0	0	0	0	0	0	0	0	34	22	2	3	18
FO4	<b>2.5</b>	0.3	0.2	0.0	221	<b>2.38</b>	0.45	182	0	0	0	0	0	0	0	0	3600*	124	19	24	82
FO7	0.0	0.0	0.0	0.0	209	0.05	0.04	209	0	0	0	0	0	0	0	0	177	116	17	19	43
FO9	<b>8.1</b>	0.4	0.3	0.1	<b>No Integer Feasible Solution Found</b>				0	0	0	0	0	0	0	0	3600*	<b>9600†</b>	84	86	114
<b>PT 191-bus ADS</b>																					
FO1	0.1	0.0	0.0	0.0	0	0	0	0	0	0	0	0	0	0	0	0	167	125	14	26	185
FO4	0.5	0.1	0.0	0.0	<b>No Integer Feasible Solution Found</b>				4	<b>2.06</b>	1.53	1	0	0	0	0	3600*	3600*	44	49	263
FO7	<b>2.4</b>	0.4	0.2	0.0	<b>No Integer Feasible Solution Found</b>				6	<b>1.43</b>	0.52	5	3	0.26	0.18	3	3600*	3600*	102	207	241
FO9	<b>3.6</b>	0.4	0.3	0.0	<b>No Integer Feasible Solution Found</b>				6	<b>2.01</b>	0.71	4	4	0.21	0.12	4	3600*	3600*	715	622	800

\*: maximum time execution limit reached in MINLP solver; †: No solution found even after 3 hours

TABLE XII  
PERFORMANCE OF MISOCP FOR FLEXIBILITY PROCUREMENT OBJECTIVE

Test Cases	FOs	Optimality Gap (%)	Constraints Violations				Maximum Relaxation Error (pu)	Time (s)	
			Nb.	Max (%)	Avg. (%)	≤ 1%			
34-bus	FO4†	100.0	2799	10.9	1.1	1952	$2.9 \times 10^{-4}$	16	15
	FO9†	100.0	2759	10.8	1.1	1964	$3.5 \times 10^{-4}$	23	15
UK 31-bus	FO4†	33.1	7440	43.9	38.1	0	$3.5 \times 10^{-3}$	3600	355
	FO9†	37.1	7440	65.9	39.1	0	$4.8 \times 10^{-3}$	3600	2671
PT 191-bus	FO4†	85.1	45840	73.2	33.5	0	$1.5 \times 10^{-3}$	3600	5597
	FO9†	70.9	45840	72.0	33.5	0	$1.4 \times 10^{-3}$	3600	13508

†: taps = 09

loading value and as such, the DSO can still use this slightly infeasible yet workable solution. Please refer to the section V-J1 which explains in detail the mindset of this paper and justifies why a slightly AC infeasible solution can be employed by a DSO.

In the case of flexibility procurement objective, it can be noticed in Table XII that MISOCP leads to an AC infeasible solution in all test cases under studied FOs due to the fact that the relaxation fails to hold as can be seen by a large value of relaxation error. On the other hand, the proposed approaches provide AC feasible solution in all cases except A1 which provides feasible solution only in the case of 34-bus and UK 31-bus ADS for these FOs (see Tables IV, VI and VIII). Nevertheless, even in those cases where A1 provides AC infeasible solution, the maximum violation remains within (1.5–3)% of the maximum overload in comparison to the (33–100)% violation recovered from MISOCP.

The presented results in Tables XI and XII clearly demonstrate that MISOCP approach fails to provide an AC feasible solution in the majority of studied cases for both objective functions as relaxation does not hold (maximum relaxation error lies in the range of  $10^{-3}$ – $10^{-4}$ ). The proposed approaches, particularly A2 and A3, on the other hand, lead to an optimal and AC feasible solution for both objective functions in all test cases, which shows clearly the superior performance of proposed approaches over state-of-the-art convex relaxation-based MISOCP methodology.

In terms of global optimality of proposed approaches solution, it can be seen in Table XI that whenever relaxation holds, i.e., in the case of UK 31-bus (FOs 1 and 7) and PT 191-bus ADS (FO1),

the recovered solution by MISOCP is indeed the global optimal solution. Since benchmark and proposed approaches solution also converge to the same optimal solution (as can be noticed by the negligible optimality gap value), it can be inferred that the solution provided by these approaches is also the global optimal. For cases where the relaxation does not hold, MISCOP only provides a lower bound to objective value, whereas proposed approaches lead to the same optimal solution as benchmark A0 approach. These results clearly demonstrate that presented approaches not only provide the global optimal solution but are also capable of providing an AC feasible solution under different objective functions and FOs where MISOCP fails to provide a meaningful solution.

Finally, in terms of computational time, the MISOCP methodology solution time increases significantly under increasing number of binary variables and quadratic constraints as can be noticed in the case of PT 191-bus ADS for FOs 4, 7 and 9. It is also observed that no integer solution is found for UK 31-bus ADS for FO 9 even after 3 hours. These results suggest that the performance of solvers for convex quadratic programs can deteriorate significantly under large problem size and as such, they might not be able able to provide a physically meaningful solution in the allotted computational time.

### I. Impact of Trustable Approximation Loop on the Accuracy of Proposed Methodologies

Table XIII presents the obtained results for all test cases under studied FOs when trustable approximation loop is discarded. Note that without trustable approximation loop, A1 reduces to single-shot linearization approach.

It can be noticed that in the case of 34-bus ADS, single-shot linearization provides an AC feasible solution but at the expense of large optimality gap (the optimality gap is ≈3.5%). In the case of UK and PT ADSs, single-shot linearization technique fails to provide an AC feasible solution as in both FOs, branch loading limits are violated. In comparison to the single-shot linearization, the proposed A1 approach provides AC feasible solution (with optimality gap less than 0.2%) in all ADSs for these FOs as shown in Tables IV, VI and VIII.

TABLE XIII  
IMPACT OF TRUSTABLE APPROXIMATION LOOP ON THE ACCURACY OF  
PROPOSED APPROACHES

FOs	Optimality Gap (%)			Constraint Violations					
				A1'			A2'		
	A1'	A2'	A3'	Nb.	Max (%)	$\leq 1$ (%)	Nb.	Max (%)	$\leq 1$ (%)
<b>34-bus ADS</b>									
FO1	3.49	0.02	0	0	$2.60 \times -4$	0	0	$2.20 \times -4$	0
FO7	2.98	0.28	0.28	0	$2.45 \times -4$	0	0	$2.45 \times -4$	0
<b>UK 31-bus ADS</b>									
FO1	0.27	0.00	0.16	8	<b>1.48</b>	6	4	0.38	4
FO7	0.51	0.15	0.00	12	<b>5.79</b>	3	9	0.26	9
<b>PT 191-bus ADS</b>									
FO1	0.37	0.01	0.10	16	<b>5.33</b>	2	16	0.64	16
FO7	0.44	0.05	0.20	15	<b>5.86</b>	1	12	0.20	12

†: taps = 09; ': Trustable approximation loop is discarded

On the other hand, in the case of A2 and A3 approaches without trustable approximation loop, AC feasible solution is obtained. However, a slightly higher optimality gap, in comparison to the case when trustable approximation loop is implemented, as shown in Tables IV, VI and VIII, is obtained.

These results clearly demonstrate that the inclusion of trustable approximation loop significantly improves the performance of all approaches, in particular, single shot linearization technique. For the latter, the trustable approximation loop not only leads to an AC feasible solution but also reduces the optimality gap, whereas for A2 and A3, the trustable approximation loop further reduces the optimality gap.

#### J. Concluding Remarks on the Selection, Accuracy, Scalability, Feasibility and Global Optimality of Proposed Approaches

This section summarizes the main findings about the performance of proposed solution approaches in terms of accuracy, solution time, feasibility and global optimality.

1) *Selection of Proposed Approaches:* A key question that arises is which among the proposed approaches can be adopted by DSO for the optimal operation of its ADSs i.e., how to quantify the trade-off between the accuracy and tractability of proposed methodologies? To answer this question, we would like to emphasize that this paper adopts an industrial application, rather than a fully academic, mindset which seeks to develop solution approaches that are able to provide the best possible solution by complying to the computational time requirements of DSOs (ideally between 15–60 minutes even in the frame of day-ahead operation planning). Furthermore, the adopted mindset shifts the focus from mathematically rigorous optimization of ideal models to efficient improvements in the allotted calculation time of imperfectly known real-world models [39]. This means that the best possible solution may not always be the global optimum or even it may (ideally slightly) violate some constraints (note that according to countries grid codes, no DSO commits to ensure the full constraint satisfaction at all time; hence sometimes some constraints such as voltage limits, may be slightly violated).

On the basis of this mindset and provided results in this paper, we emphasize that the selection of a particular approach can be decided by a DSO by considering its accuracy and computational time requirements, as well as taking into account the context (amount and type of DER, uncertainty scenarios, time resolution), network particularities (large scale, radial, mesh) and solution time constraints. For instance, DSO can opt for A3 for increased accuracy under less stringent solution time constraint and small-medium size ADS. However, if the computation time of A3 becomes an issue, A2 can come into play as it is the best trade-off between accuracy and speed. Lastly, for extremely large size problem where the sole priority of DSO is to have a solution in the allotted time, A1 becomes the necessary choice at the expense of (possibly) less precision.

2) *Accuracy of Proposed Approaches:* The proposed solution approaches provide AC feasible and optimal solution for all FOs in all test cases under normal operating conditions. Among the proposed approaches, A2 and A3 outperform A1 in terms of solution accuracy by further reducing the optimality gap. On the other hand, under stressed operating conditions, A2 and A3 still lead to an optimal and AC feasible solution, whereas there exist a few instances where A1 provides a slightly infeasible solution. However, it is important to emphasize that reducing the thermal limit by 20% is a very demanding case (given that the congestion already appears in the base case). Even under such scenario, the branch overloading remains below 3% in the case of A1 and this slightly infeasible solution can still be employed by DSOs in the mindset of this paper. Based on these results, it can, therefore, be safely concluded that all solution approaches, in particular A2 and A3, are capable of providing a highly accurate solution under normal and stressed operating conditions.

3) *Feasibility of Proposed Approaches:* Approach A3 always provides an AC feasible solution provided it converges. On the other hand, A1 and A2 solve an approximated OPF problem and as such, AC feasibility of the obtained solution needs to be determined. The vast numerical simulations show that A2 (almost) always leads to an AC feasible solution, whereas approach A1 provides an AC infeasible solution only in few cases under stressed operating conditions. Under normal operating conditions, A1 leads to an AC feasible solution.

The presented results also demonstrate that the performance of A1 without trustable approximation loop (A1 is widely studied single shot linearization approach when trustable approximation loop is discarded as previously reported) deteriorates significantly. This shows that the single shot linearization approach, which works well in the vicinity of its point of linearization, might fail under stressed operating conditions and leads to an AC infeasible solution. As such, the addition of trustable approximation loop not only extends the state-of-the-art (i.e., single shot linearization) but also increases the accuracy of the latter, thus leading to an AC feasible solution.

Finally, it is important to mention that under the scenario where approach A1 leads to an AC infeasible solution, no attempt is made to correct the A1 solution. The rationale behind keeping/utilizing the AC infeasible solution lies in the mindset of this paper i.e., under stringent solution time requirements, A2 and A3 might not be able to provide a solution at all for

large problem size. Under such circumstances, A1 becomes the necessary choice for DSOs as it is able to provide a solution, which can be, but not necessarily, slightly AC infeasible, in the allotted time requirements and as such, a slightly infeasible yet workable solution is better for DSOs than no solution.

*4) Global Optimality of Proposed Approaches Solution:* Regarding the global optimality of obtained solution from benchmark A0 and proposed approaches (A1, A2 and A3), it can be cautiously concluded that the presented approaches provide the global optimal solution as the same optimal solution is obtained by the convex MISOCP whenever relaxation holds. On the other hand, whenever relaxation does not hold, one can still consider the solution obtained from the presented techniques as the global optimum since extensive numerical evidence, presented in [40] and this paper, also points out that the solution provided by a local optimizer (e.g., IPOPT) is global optimum in most generic AC OPF problem instances. Based on this, it can be deduced that the probability of obtaining the global optimum from A0 approach is high and as such, the close vicinity of approach A1, A2 and A3 solution to the A0 solution makes it global optimum as well.

*5) Scalability of Proposed Approaches:* In terms of computational performance, A1 and A2 take almost the same amount of time in the case of small-size ADSs, whereas in the case of large size ADSs, the solution time of A2 increases slightly as compared to the solution time of A1. Nevertheless, both approaches A1 and A2 solution time remains compatible with the day-ahead operation planning requirements and both approaches are scalable for large size ADSs. On the other hand, the proposed approach A3 takes significant amount of time in comparison to the A1 and A2 due to the fact that a non-convex NLP problem is solved in A3. As such, approach A3 can be adopted in cases where solution accuracy cannot be compromised at the expense of a large computational time.

## VI. CONCLUSION

This paper has proposed three novel fast tailored approaches (A1, A2, A3), which comply with the stringent solution time requirement of DSOs, to solve S-MP-OPF MINLP problems for day-ahead flexibility procurement from DER in active distribution systems. The proposed approaches share a first common recursive MILP approximation step, which relies on a new linear approximations of AC power flows and branch current expressions. This step fixes also all binary variables in the problem while the subsequent steps further refine the values of continuous variables. Then, A1 uses MILP and AC feasibility check, A2 employs MILP, SLP and AC feasibility check, while A3 relies on MILP and NLP.

Extensive numerical results for three different networks and various problem instances as combinations of flexibility options demonstrate empirically that the approach A2 provides the best trade-off between accuracy and speed. Indeed, in terms of solution accuracy, the approach A2 provides an optimal and AC feasible solution, except one instance (out of 33) where the solution is slightly infeasible (one limit is violated by 1.14%).

Despite the main conclusion, the pros and cons of the approaches should be nuanced: the trade-offs between solution accuracy and tractability of the proposed approaches may make any of them more suitable in a certain context. For instance, the approach A3 can be preferred, at the expense of significantly larger computation time, whenever stringent AC feasibility is required at all times.

The approaches A1 and A2 scale well with the problem size and their computation effort is compatible with application requirements in day-ahead operation planning. Their applicability to even larger networks can be safely envisioned. The results have also shown that the fastest approach A1, which adopts the widely-used single-step problem linearization, can produce infeasible solutions under stressed operating conditions. On the other hand, AC-feasible solution is obtained in the approach A2 within few SLP iterations as well as the accuracy of developed linear approximations remains intact under tougher operation conditions.

To conclude, the proposed approaches (A1, A2 and A3) are reasonable and sophisticated heuristics, with A2 and A3 presenting excellent empirical evidence of ability to lead an accurate, feasible and optimal solution, whereas A1 presents the ability of providing a solution under stringent time requirements where A2 and A3 might fail to provide any solution.

Last but not least, the numerical results show that the proposed approaches outperform a benchmark MINLP solver and a state-of-the-art method from the literature as thoroughly compared in three radial or weakly meshed ADSs of 34, 31, and 191 nodes, respectively. The numerical results indicate that, albeit the approach A2 performs best overall, these approaches present distinct accuracy vs speed trade-offs, which make them suitable to problems of different sizes and diverse accuracy or speed requirements.

Lastly, an open research question is whether the proposed linearization may be leveraged to applications, such as AC OPF or unit commitment, in other meshed transmission grid.

## REFERENCES

- [1] A. Keane et al., "State-of-the-art techniques and challenges ahead for distributed generation planning and optimization," *IEEE Trans. Power Syst.*, vol. 28, no. 2, pp. 1493–1502, May 2013.
- [2] M. Usman, M. Coppo, F. Bignucolo, and R. Turri, "Losses management strategies in active distribution networks: A review," *EPSR*, vol. 163, pp. 116–132, 2018.
- [3] M. Usman and F. Capitanescu, "A stochastic multi-period AC OPF for provision of flexibility services in smart grids," in *Proc. IEEE PowerTech*, Madrid, Spain, 2021, pp. 1–6.
- [4] F. U. Nazir, B. C. Pal, and R. A. Jabr, "A two-stage chance constrained volt/var control scheme for active distribution networks with nodal power uncertainties," *IEEE Trans. Power Syst.*, vol. 34, no. 1, pp. 314–325, Jan. 2019.
- [5] T. Ding, C. Li, Y. Yang, J. Jiang, Z. Bie, and F. Blaabjerg, "A two-stage robust optimization for centralized-optimal dispatch of photovoltaic inverters in active distribution networks," *IEEE Trans. Sustain. Energy*, vol. 8, no. 2, pp. 744–754, Apr. 2017.
- [6] T. Ding, S. Liu, W. Yuan, Z. Bie, and B. Zeng, "A two-stage robust reactive power optimization considering uncertain wind power integration in active distribution networks," *IEEE Trans. Sustain. Energy*, vol. 7, no. 1, pp. 301–311, Jan. 2016.
- [7] M. Bazrafshan and N. Gatsis, "Decentralized stochastic optimal power flow in radial networks with distributed generation," *IEEE Trans. Smart Grid*, vol. 8, no. 2, pp. 787–801, Mar. 2017.

- [8] Q. Gemine, E. Karangelos, D. Ernst, and B. Cornélusse, "Active network management: Planning under uncertainty for exploiting load modulation," in *Proc. IEEE IREP Symp. Bulk Power Syst. Dyn. Control - IX Optim., Secur. Control Emerg. Power Grid*, 2013, pp. 1–9.
- [9] G. Zou, Y. Ma, J. Yang, and M. Hou, "Multi-time scale optimal dispatch in ADN based on MILP," *Int. J. Electr. Power Energy Syst.*, vol. 102, pp. 393–400, 2018.
- [10] S. Gill, I. Kockar, and G. W. Ault, "Dynamic optimal power flow for active distribution networks," *IEEE Trans. Power Syst.*, vol. 29, no. 1, pp. 121–131, Jan. 2014.
- [11] A. Gabash and P. Li, "Active-reactive optimal power flow in distribution networks with embedded generation and battery storage," *IEEE Trans. Power Syst.*, vol. 27, no. 4, pp. 2026–2035, Nov. 2012.
- [12] V. A. Evangelopoulos, I. I. Avramidis, and P. S. Georgilakis, "Flexibility services management under uncertainties for power distribution systems: Stochastic scheduling and predictive real-time dispatch," *IEEE Access*, vol. 8, pp. 38855–38871, 2020.
- [13] T. Soares, R. J. Bessa, P. Pinson, and H. Morais, "Active distribution grid management based on robust AC optimal power flow," *IEEE Trans. Smart Grid*, vol. 9, no. 6, pp. 6229–6241, Nov. 2018.
- [14] A.A. Ejajal, M. F. Shaaban, K. Ponmambalam, and E. El-Saadany, "Stochastic centralized dispatch scheme for AC/DC hybrid smart distribution systems," *IEEE Trans. Sustain. Energy*, vol. 7, no. 3, pp. 1046–1059, Jul. 2016.
- [15] H. Gao, J. Liu, and L. Wang, "Robust coordinated optimization of active and reactive power in active distribution systems," *IEEE Trans. Smart Grid*, vol. 9, no. 5, pp. 4436–4447, Sep. 2018.
- [16] X. Yang, C. Xu, H. He, W. Yao, J. Wen, and Y. Zhang, "Flexibility provisions in active distribution networks with uncertainties," *IEEE Trans. Sustain. Energy*, vol. 12, no. 1, pp. 553–567, Jan. 2021.
- [17] E. Dall'Anese, K. Baker, and T. Summers, "Chance-constrained AC optimal power flow for distribution systems with renewables," *IEEE Trans. Power Syst.*, vol. 32, no. 5, pp. 3427–3438, Sep. 2017.
- [18] A. Baharvandi, J. Aghaei, A. Nikoobakht, and others, "Linearized hybrid stochastic/robust scheduling of active distribution networks encompassing PVs," *IEEE Trans. Smart Grid*, vol. 11, no. 1, pp. 357–367, Jan. 2020.
- [19] A. N. Toutounchi, S. Seyedshenava, J. Contreras, and A. Akbarimajd, "A stochastic bilevel model to manage active distribution networks with multi-microgrids," *IEEE Syst. J.*, vol. 13, no. 4, pp. 4190–4199, Dec. 2019.
- [20] J. Soares, M. A. F. Ghazvini, N. Borges, and Z. Vale, "A stochastic model for energy resources management considering demand response in smart grids," *EPSR*, vol. 143, pp. 599–610, 2017.
- [21] J. G. Robertson, G. P. Harrison, and A. R. Wallace, "OPF techniques for real-time active management of distribution networks," *IEEE Trans. Power Syst.*, vol. 32, no. 5, pp. 3529–3537, Sep. 2017.
- [22] L. Gan and S. H. Low, "An online gradient algorithm for optimal power flow on radial networks," *IEEE J. Sel. Areas Commun.*, vol. 34, no. 3, pp. 625–638, Mar. 2016.
- [23] E. Dall'Anese and A. Simonetto, "Optimal power flow pursuit," *IEEE Trans. Smart Grid*, vol. 9, no. 2, pp. 942–952, Mar. 2018.
- [24] S. Bolognani and S. Zampieri, "On the existence and linear approximation of the power flow solution in power distribution networks," *IEEE Trans. Power Syst.*, vol. 31, no. 1, pp. 163–172, Jan. 2016.
- [25] S. H. Low, "Convex relaxation of optimal power flow—Part II: Exactness," *IEEE Trans. Control Netw. Syst.*, vol. 1, no. 2, pp. 177–189, Jun. 2014.
- [26] Z. Yang, K. Xie, J. Yu, H. Zhong, N. Zhang, and Q. Xia, "A general formulation of linear power flow models: Basic theory and error analysis," *IEEE Trans. Power Syst.*, vol. 34, no. 2, pp. 1315–1324, Mar. 2019.
- [27] J. Yang, N. Zhang, C. Kang, and Q. Xia, "A state-independent linear power flow model with accurate estimation of voltage magnitude," *IEEE Trans. Power Syst.*, vol. 32, no. 5, pp. 3607–3617, Sep. 2017.
- [28] S. M. Fatemi, S. Abedi, G. Gharehpetian, S. H. Hosseiniyan, and M. Abedi, "Introducing a novel DC power flow method with reactive power considerations," *IEEE Trans. Power Syst.*, vol. 30, no. 6, pp. 3012–3023, Nov. 2015.
- [29] T. Akbari and M. T. Bina, "Linear approximated formulation of AC optimal power flow using binary discretisation," *IET GTD*, vol. 10, no. 5, pp. 1117–1123, 2016.
- [30] M. Usman and F. Capitanescu, "A new second-order linear approximation to AC OPF managing flexibility provision in smart grids," in *Proc. IEEE Int. Conf. Smart Energy Syst. Technologies*, 2021, pp. 1–6.
- [31] W. Wu, Z. Tian, and B. Zhang, "An exact linearization method for OLTC of transformer in branch flow model," *IEEE Trans. Power Syst.*, vol. 32, no. 3, pp. 2475–2476, May 2017.
- [32] W. Wei, "Tutorials on advanced optimization methods," *arXiv: 2007.13545*.
- [33] P. Li et al., "Coordinated control method of voltage and reactive power for active distribution networks based on soft open point," *IEEE Trans. Sustain. Energy*, vol. 8, no. 4, pp. 1430–1442, Oct. 2017.
- [34] Z. Yang, H. Zhong, A. Bose, T. Zheng, Q. Xia, and C. Kang, "A linearized OPF model with reactive power and voltage magnitude: A pathway to improve the MW-only DC OPF," *IEEE Trans. Power Syst.*, vol. 33, no. 2, pp. 1734–1745, Mar. 2018.
- [35] M. E. Baran and F. F. Wu, "Network reconfiguration in distribution systems for loss reduction and load balancing," *IEEE Power Eng. Rev.*, vol. 4, no. 2, pp. 1401–1407, Apr. 1989.
- [36] Open data sets from ATTEST project. [Online]. Available: <https://zenodo.org/communities/attest-eu/?page=1&size=20>
- [37] I. Dunning, J. Huchette, and M. Lubin, "JuMP: A modeling language for mathematical optimization," *SIAM Rev.*, vol. 59, no. 2, pp. 295–320, 2017.
- [38] S. E. Kayacik and B. Kocuk, "An MISOCP-based solution approach to the reactive optimal power flow problem," *IEEE Trans. Power Syst.*, vol. 36, no. 1, pp. 529–532, Jan. 2021.
- [39] F. Capitanescu, "Suppressing ineffective control actions in optimal power flow problems," *IET Gener. Transmiss. Distribution*, vol. 14, no. 13, pp. 2520–2527, Jul. 2020.
- [40] C. Coffrin, H. L. Hijazi, and P. Van Hentenryck, "The QC relaxation: A theoretical and computational study on optimal power flow," *IEEE Trans. Power Syst.*, vol. 31, no. 4, pp. 3008–3018, Jul. 2016.



**Muhammad Usman** (Member, IEEE) received the Master of Science degree in power engineering from the Technical University of Munich, Munich, Germany, in 2016, and the Ph.D. degree in electrical energy engineering from the University of Padova, Padua, Italy, in 2020. His main research interests include the modeling and analysis of medium- and low-voltage active distribution systems through optimization techniques, particularly single- and multi-phase optimal power flow approach, and losses allocation, for smart grid management.



**Florin Capitanescu** (Member, IEEE) received the Electrical Power Engineering degree from the Politehnica University of Bucharest, Bucharest, Romania, in 1997, and the Ph.D. degree from the University of Liège, Liège, Belgium, in 2003. Since 2015, he has been a Senior Researcher with the Luxembourg Institute of Science and Technology, Esch-sur-Alzette, Luxembourg. His main research interests include the application of optimization methods to the operation of transmission and active distribution systems, particularly optimal power flow approaches, power systems security, voltage instability, and smart sustainable buildings.